Spanish Journal of Agricultural Research
19 (2), e0301, 14 pages (2021)
eISSN: 2171-9292
https://doi.org/10.5424/sjar/2021192-17112
Instituto Nacional de Investigación y Tecnología Agraria y Alimentaria (INIA)

RESEARCH ARTICLE

OPEN ACCESS

Modelling the impacts of climate change on potential cultivation area and water deficit in five Mediterranean crops

Anton Montsant[1], Oriol Baena[1], Lluís Bernàrdez[2] and Jordi Puig[1]

[1] *Espigall, Alzina 23, 08480 L'Ametlla del Vallès, Barcelona, Spain* [2] *Gauss School of Mathematics, Antic Camí de Caldes 1B, 08480 L'Ametlla del Vallès, Barcelona, Spain*

Abstract

Aim of study: To assess the impacts of climate change on local agriculture with a high resolution in a Mediterranean region with a diversity of climates.

Area of study: Catalonia (NE Spain).

Material and methods: Based on historical meteorological records and a regionalization of the RCP4.5 model created by the Catalan Meteorological Service, the Papadakis agro-climate classification was calculated for two climate scenarios. The changes in agro-climatic suitability and irrigation needs of five typical Mediterranean crops (alfalfa, almond, barley, olive and orange) were analysed.

Main results: In the 2031-2050 climate scenario, over 15% of the study area will no longer be adequate for non-irrigated almond or olive, at locations in which they have been traditionally rainfed crops. If irrigation is provided, orange is likely to become agro-climatically suited for the entire Catalan coastline. Were the current crop distribution maintained, irrigation needs may increase on average 16% in the study area in the future scenario.

Research highlights: High-resolution GIS data may be combined with Papadakis' classical method to compare different climate scenarios and detect risks and opportunities for local and regional agriculture.

Additional key words: irrigation; Papadakis; agroclimate; rainfed agriculture; potential distribution

Abbreviations used: Alt (Altitude); CosLat (Cosine of Latitude); DCAC (Digital Climate Atlas of Catalonia); DistSea (Distance to the sea); DUN (*Declaració Única Agrària*, Catalan for Single Agrarian Declaration); NV (not viable); P (precipitation); Rad (radiation); Tmax (monthly average of maximum daily temperature); tmin (monthly average of minimum daily temperature); tminabs (absolute minimum daily temperature in a month); TRCC (Third Report on Climate Change in Catalonia); UK (universal kriging); V (viable); V_{irr} (viable with irrigation).

Authors' contributions: Conceived the methodology: AM, JP, OB. Acquired, analysed and interpreted data: AM, JP, LB, OB. Performed statistical analysis: AM, LB. Prepared the original draft: AM. Critically reviewed the manuscript: JP, OB. Supervised and coordinated the project: JP.

Citation: Montsant, A; Baena, O; Bernàrdez, L; Puig, J (2021). Modelling the impacts of climate change on potential cultivation area and water deficit in five Mediterranean crops. Spanish Journal of Agricultural Research, Volume 19, Issue 2, e0301. https://doi.org/10.5424/sjar/2021192-17112

Supplementary material: (Fig. S1 and Tables S1 to S7) accompanies the paper on SJAR's website

Received: 30 Jun 2020. **Accepted:** 17 May 2021.

Funding: The authors received no specific funding for this work

Competing interests: The authors have declared that no competing interests exist.

Correspondence should be addressed to Jordi Puig: jordi@espigall.cat

Introduction

Catalonia (NE Spain) is a region located on the north-western Mediterranean coast with a contrasting terrain that generates a great diversity of microclimates. The Pyrenees and the smaller mountain ranges that extend parallel to the coastline have determined distinct bioregions with a characteristic climate, natural vegetation and traditional crops. The total area of Catalonia is 31,895 km^2, of which 26% is agricultural land, 64% is forest, and the rest is urban regions and other land uses. Traditionally, the coastal strip has been an area of dryland agriculture based on crops with a low water demand (hereafter 'Littoral subregion'). Inland, there is a very dry area where irrigation is predominant ('Interior subregion'), and then finally there is the mountain climate zone ('Pyrenees subregion') dedicated to pastures, forestry, and crops with higher water demands (forage and some fruit and vegetable species) (Fig. 1).

The impact of climate change on this complex landscape is already underway (Peñuelas & Boada, 2003; Pascual *et al.*, 2016). Numerous studies predict a

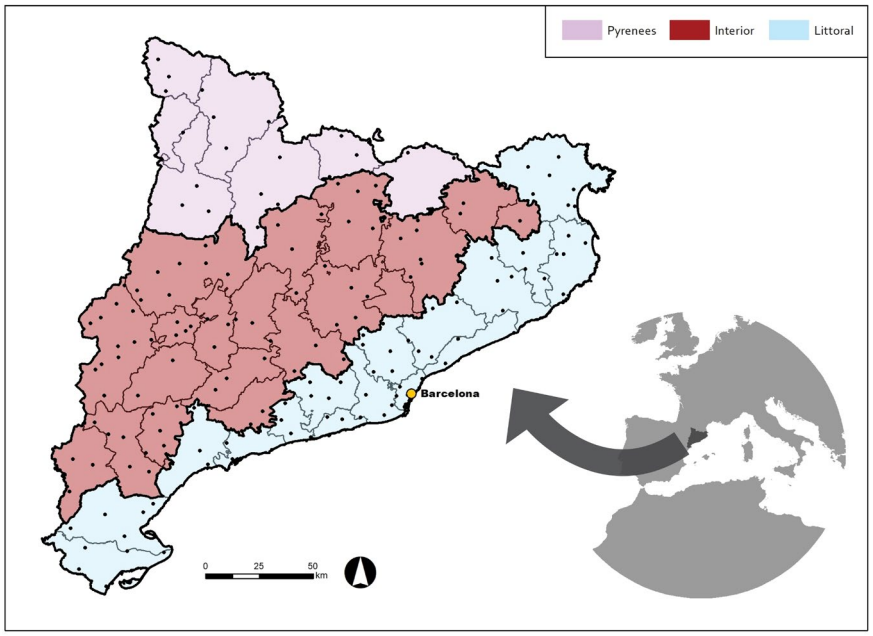

Figure 1. Situation of the study area, showing the three traditional agricultural and climatic subregions. Black dots indicate the location of meteorological stations

change to warmer conditions and an increase in water deficit for the North-western Mediterranean coast (Quiroga & Iglesias, 2009; Tanasijevic *et al.*, 2014; Donatelli *et al.*, 2015), and the future performances of specific crops have been modelled with a broad regional scope (Garrido *et al.*, 2011; Ferrise *et al.*, 2013; Saadi *et al.*, 2015). However, local studies are needed to promote the optimal adaptation strategies for the agricultural sector of each territory in a changing environment, a process that should be championed and monitored by local administrations and local farmers organizations (Ronchail *et al.*, 2014).

In this article, we aimed to quantify the impacts of climate change predictions on traditional rainfed species and identify the regions in which crop replacement or irrigation developments will be required. To measure these impacts, we used Papadakis' agroclimatic classification with a high spatial resolution in Catalonia. The modifications that this agroclimatic zoning will experience according to regional projections of climate change were calculated. The impacts of these modifications on five important Mediterranean crops, which added up to 44.9% of the arable land of Catalonia in 2018, were analysed. Alfalfa (*Medicago sativa*; 4.5% of total arable land) and barley (*Hordeum vulgare*; 23.6%) served as models for rainfed herbaceous crops traditionally produced in the more humid or in dry Mediterranean areas, respectively. Almond (Prunus dulcis; 4.6%) and olive (*Olea europaea*; 12.0%) have been the most common rainfed woody crops for centuries in the study area. However, modern commercial agriculture requires constant high productivities, and so irrigation has been implemented where possible also for these four crops. Finally, orange (*Citrus* × *sinensis*; 0.2%) was studied as a crop with a great expansion potential in irrigated conditions. Oranges are successfully produced in the southern warm areas of Catalonia, and are a traditional local product in Valencia, which is immediately to the south. Orange is therefore likely to expand its agroclimatic viability northwards as winters expectedly become milder.

Material and methods

Retrieval of public geographic and climate data

Papadakis' classification is based on a calculation cascade starting with four monthly values (48 variables in total): monthly average of daily minimum temperature (tmin, ºC) and maximum temperature (Tmax, ºC), average monthly precipitation (P, mm/month), and average absolute minimum temperature of every month (tminabs). The first three types of values (36 variables) are publicly available from the Digital Climate Atlas of Catalonia (DCAC) as data layers in raster format with a resolution of 180 m, derived from meteorological records (Ninyerola *et al.*, 2000). For every location of this grid, altitude (Alt, meters above the sea level), distance to the sea (DistSea, km), the latitude expressed as a cosine (CosLat), UTM coordinates, and monthly data of average solar radiation (Rad, 10 $kJ \cdot m^{-2} \cdot day^{-1}$) were obtained in order to calculate tminabs following the methodology of the publicly available temperature data layers. All data were extracted with QGIS v3.10.

Generation of monthly absolute minimum temperature layers from meteorological records

The Catalan Meteorological Service provided tminabs data of 151 meteorological stations spanning a minimum of 12 years (2007-18). The locations of these stations are indicated in Fig. 1. For these 12-year series the average tminabs of every month were calculated, and multiple linear regressions were performed to obtain average tminabs as a function of four independent variables (Alt, CosLat, DistSea, and Rad).

$$z(s) = \beta + \sum_{k=1}^{p} \alpha_k \cdot f_k(s) \quad (1)$$

where z (*s*) is tminabs at location *s*, β is the intercept, $f_k(s)$ are the four independent variables and α_k are the regression coefficients of the independent variables.

Subsequently, average monthly tminabs values were obtained throughout the study area using the Universal Kriging (UK) interpolation method:

$$z(s) = \beta + \sum_{k=1}^{p} \alpha_k \cdot f_k(s) + \sum_{i=1}^{q} \lambda_i \cdot \varepsilon(s_i) \quad (2)$$

where λ_i are kriging weights and $\varepsilon(s_i)$ is the observed residual at measurement locations s_i. Further details are readily available in the literature (Benavides *et al.*, 2007; Hengl *et al.*, 2007; Bostan *et al.*, 2012). For each month, the UK interpolation was performed using only the variables that proved significant in the multiple regression (Rad was found to be not significant for some of the months, see Results). Therefore, the value p is 3 or 4 depending on the number of significant variables, while q=151 meteorological stations.

For both kriging and regression, models were validated by initially using 66.6% of the data (100 stations) and contrasting the results with the remaining 33.4%. Root-mean-square errors (RMSE) were calculated by comparing predictions for the meteorological station sites with the actual observed values (20 random iterations).

$$RMSE = \sqrt{\frac{\sum_{i=1}^{n}(O_i - P_i)^2}{n}} \quad (3)$$

where O_i=observed value based on meteorological station records; P_i=predicted value by either kriging or linear regression. To obtain the final layers of monthly tminabs, data from all 151 stations were used. All computations were developed with the statistical package R Studio v1.2.50001.

Baseline (1971-2000) and future (2031-2050) scenarios under study

The Third Report on Climate Change in Catalonia (TRCCC) offers estimates of temperature and precipitation changes for the 2012-2020 and 2031-50 time periods (relative to the period 1971-2000, hereafter "baseline scenario"). These estimations were based on a regionalization of the RCP4.5 emissivity scenario (Calbó *et al.*, 2016). In the TRCCC, the expected percent variation of precipitation and average temperature increase were calculated in a subregion- and season-dependent manner (Table 1). In the present study, data layers of monthly precipitations and temperatures were obtained for the period 2031-2050 (hereafter termed "future scenario") based on these TRCCC projections:

$$T_x(2031) = T_x(1971) + K_t^{2031} \quad (4)$$

$$P(2031) = (1 + K_p^{2031}) * P(1971) \quad (5)$$

Table 1. Constants used to transform temperature and precipitation values among baseline and future scenarios (temperature variation in °C and precipitation change in %) as reported in the Third Report on Climate Change in Catalonia (Calbó *et al.*, 2016).

	2012-2021 *vs* 1971-2000	**Winter**	**Spring**	**Summer**	**Autumn**
Littoral	Temperature (ºc)	0.6	0.7	0.9	0.8
	Precipitation (%)	-5.4	-6.4	-1.9	-7.9
Interior	Temperature (ºc)	0.6	0.8	0.9	0.8
	Precipitation (%)	2.3	-5.9	-1.6	-4.3
Pyrenees	Temperature (ºc)	0.7	0.8	0.9	0.7
	Precipitation (%)	2.7	-0.8	-2.5	-2.7
	2031-2050 *vs* 1971-2000	**Winter**	**Spring**	**Summer**	**Autumn**
Littoral	Temperature (ºc)	1.2	1.2	1.8	1.7
	Precipitation (%)	-6	-12.0	-11.7	-9.1
Interior	Temperature (ºc)	1.2	1.2	1.9	1.7
	Precipitation (%)	-1.1	-11.5	-9.9	-8.9
Pyrenees	Temperature (ºc)	1.4	1.4	1.9	1.8
	Precipitation (%)	-1.8	-8.4	-9.0	-9.3

where T_x=Tmax or tmin; K_t^{2031}=temperature variation constant (as ºC) for the 2031-2050 scenario, for the corresponding month and subregion (Table 1); K_p^{2031}=precipitation variation constant (as %) for the 2031-2050 scenario, for the corresponding month and subregion (Table 1).

The limits of the three subregions in which Catalonia was divided are depicted in Fig. 1.

On the other hand, public datasets of Tmax, tmin, and P are based on meteorological records that cover the baseline scenario, but no tminabs datasets are available for this period. Since the tminabs layers calculated in this study are based on data from years 2007-2018, they were considered to correspond to the 2012-2021 scenario, so the variation constants between the baseline and the 2012-2021 scenarios were subtracted to generate simulated tminabs data for the baseline scenario.

$$\text{tminabs (1971)} = \text{tminabs (2012)} - K_t^{2012} \quad (6)$$

where K_t^{2012}=temperature variation constant (as ºC) for the 2012-2021 scenario, for the corresponding month and subregion (Table 1).

Computing agroclimate according to Papadakis' classification

The methodology developed by Papadakis (1966) classifies the world's climates in terms of their agricultural potential. This classification reflects thermal and humidity regimes in detail because it uses elaborate definitions and extreme values rather than direct average parameters (Verheye, 2008). To characterize climates in terms of crop ecophysiology at a specific location, Papadakis' procedure takes into account winter severity, summer thermal stress, and water availability throughout the year (Fig. 2B). It uses extreme temperatures, intra-seasonal thermal and rainfall differences and soil water balance.

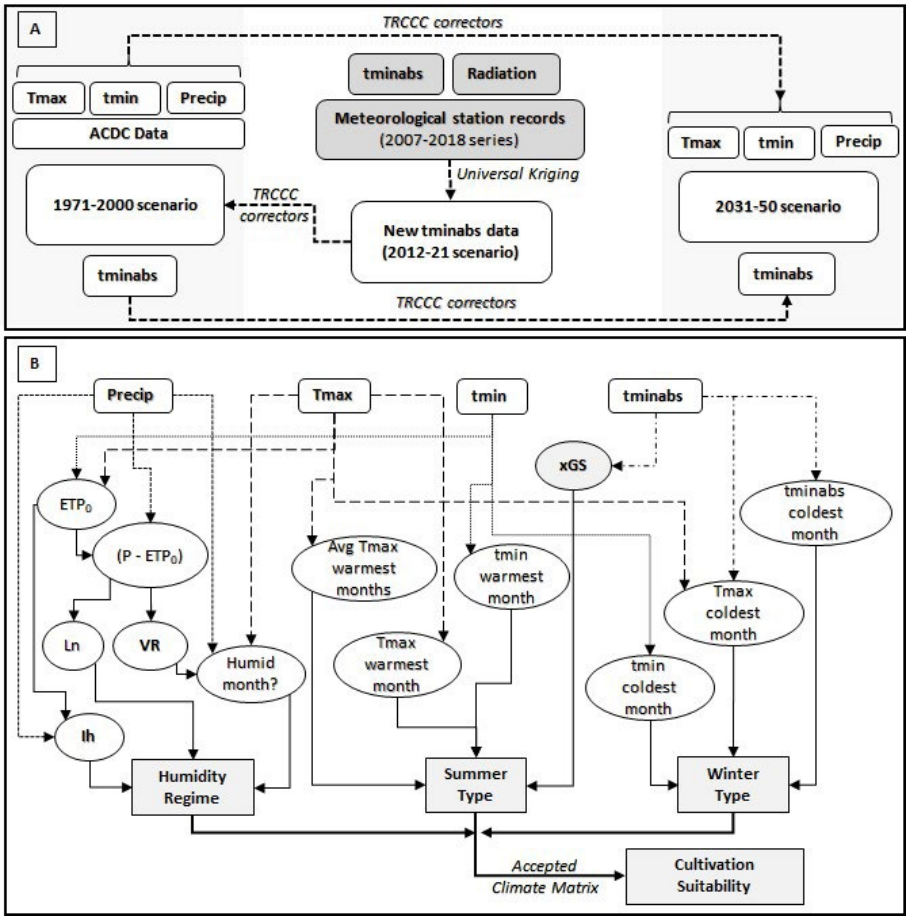

Figure 2. Flow diagram of the programming developed in spreadsheets to obtain the cultivation suitability of five crops. A) Manipulation of the available starting data to generate values of the four variables for three baseline and future scenarios through the correctors shown in Table 1. B) Calculation of agroclimatic categories according to Papadakis and resulting suitability of cultivation, performed for the baseline and future scenarios. ETP_0=potential evapotranspiration; Ln=rainwash index; I_h=humidity index; VR=variation of soil water reservoir; xGSs=growing seasons.

Winter type

The winter type defines the severity of the cold season as a function of the following parameters:

- absolute minimum temperature of the coldest month,
- minimum temperature of the coldest month,
- maximum temperature of the coldest month.

Summer type

To define the summer type, the following parameters were considered:

- Growing seasons (xGS): They are defined as the period in which temperatures are above a threshold of 0 ºC (mean GS - MGS), 2 ºC (available GS - AGS) or 7 ºC (minimum GS - minGS) at all times. To calculate them, linear regressions are made between tminabs (y axis) and months (x axis) for the two semesters of the year.

$$z\,(m_1)=\beta_1 + \alpha_1 \cdot m_1 \quad (7)$$

$$z\,(m_2)=\beta_2 + \alpha_2 \cdot m_2 \quad (8)$$

where z (m) is tminabs for month m and the subscripts indicate the semester of the regression. By making z=0, isolating m_1 and m_2 and subtracting eq (8) – eq (7), MGS is obtained. Similarly, for z=2 and z=7, the subtraction will yield AGS and minGS. It should be noted that, following Papadakis' protocol, in the semester in which monthly tminabs increases (1st semester in the Northern hemisphere), tminabs is considered to occur at the beginning of the month, while in the semester with decreasing monthly tminabs, it is considered to occur at the end of the month.

- Average of the Tmax of the n warmest months, for n=2, 4 or 6,
- Highest Tmax,
- tmin of the month with the highest Tmax,
- Average of the tmin of the two months with highest Tmax.

Humidity regime

To describe the water availability that climate provides, Papadakis' method assumed a maximum soil water content of 100 mm in the most humid month of the year. This volume is the reservoir that suffers losses due to evapotranspiration and receives input from rainfall, and a monthly water balance is performed. In the study area, this month was set as December, after the autumn rains and when day length and mean temperatures drop.

$$R_m=R_{m-1} + (P - ETP_0)_{m-1} \quad (9)$$

where R_m is the mean soil water content for month m.

The following parameters must be taken into account in order to determine the humidity regime:

- Annual humidity index (I_h): ratio of annual precipitation over evapotranspiration

$$I_h=P/ETP \quad (10)$$

- Level of humidity of every month:

If $P_m + \Delta R_m > ETPm$ → Humid month
If $P_m + \Delta R_m < 0.5*ETPm$ → Dry month

where $\Delta R_m=R_m - R_{m-1}$ is the monthly variation of soil water content.

- Rainwash index (L_n): Sum of the balance (P_m-ETP_m) over the 12 months, for all months in which $P_m>ETP_m$

$$L_n= \sum_{m=1}^{12}(P_m - ETP_m) \quad \text{for all m in which } (P_m>ETP_m) \quad (11)$$

The criteria to define each category are provided as supplementary material (Table S1 [suppl.]). Papadakis' work included the description of the climate requirements of common crops in terms of his agroclimatic classification (Table S2 [suppl.]). All maps were plotted by means of the qGIS software.

Suitability of cultivation

To quantify and visualize the impact of climate change on agriculture, five typical Mediterranean crops (almonds, olives, barley, alfalfa and oranges) were selected. Winter and summer types and humidity regimes under which the most common crops can thrive are easily available, for example from the Spanish Ministry of Agriculture (De León Llamazares, 1989; Table S2 [suppl.]). For each species, the coldest winter types and summer types that are entirely tolerated are indicated, along with excess heat constraints; from these data, a list of acceptable categories is derived. Similarly, the minimum humidity regime required by each species gives rise to a list including that level of moisture or higher.

The suitability of cultivation was computed with a logical algorithm. For each crop, every location was classified according to its ability to withstand temperature and water availability conditions at each location: viable (V), all three parameters (winter and summer types and humidity regime) allow cultivation of the variety; not viable (NV), at least one of the thermal parameters (type of summer or type of winter) is not adequate; and viable

with irrigation (V_{irr}), the humidity regime does not grant a sufficient amount of water to ensure optimal productivity, but the thermal conditions are adequate.

Adequacy of Papadakis' methodology based on present-day crop occurrence

To evaluate the fitness of the methodology developed by Papadakis to predict the agricultural potential of a region's climate with high-resolution data, the types of winter and summer of each location in which either of the five target species are present today were checked against the list of tolerated climate types of the corresponding species. Ideally, all present-day crops should be placed in locations with climate regimes that they can tolerate, and none of them should be found in areas with a climate in which they cannot thrive. To perform this analysis, the 2012-2020 agroclimatic scenario was generated by means of the variation constants shown in Table 1. The suitability of the humidity regime or presence of irrigation systems were not taken into account, because crops can hardly be present in areas that are too cold or too warm for them; however, some may exist in places that are too dry but have unregistered irrigation support, and some others may be grown in irrigated fields even if they could be grown as rainfed crops, just because water supply is readily available. Therefore, the rate of coincidence between "Papadakis climate suitability prediction" and "presence of a crop" was calculated using the type of summer and type of winter at each location only.

Water deficit

The water deficit (WD) of all five crops was calculated for every month by multiplying the K_c crop constant by monthly potential evapotranspiration (ETP_0) (Allen *et al.*, 1998), and subsequently obtaining the balance between culture evapotranspiration and effective rainfall.

$$WD = (ETP_0)_m * K_c - (P_{ef})_m \quad (12)$$

Following Papadakis' methodology, monthly ETP_0 was calculated as

$$(ETP_0)_m = 5.625 * (e_{Tmax} - e_{tmin})_m \quad (13)$$

where e_{Tmax} and e_{tmin} are the vapor pressures corresponding to Tmax or tmin in every month:

$$e_{Tx} = (33.8639 * ((0.00738*Tx+0.8072)^8 - 0.000019 * (1.8*Tx+48) + 0.001316) \quad (14)$$

Monthly effective precipitation $(P_{ef})_m$ was calculated according to Brouwer & Heibloem (1986):

$$(P_{ef})_m = 0.8 * P - 25 \quad \text{for } P_m > 75 \text{ mm} \quad (15)$$

$$(P_{ef})_m = 0.6 * P - 10 \quad \text{for } P_m < 75 \text{ mm} \quad (16)$$

K_c constants were obtained from the FAO repository (FAO, 2002) except for olive (Pastor & Orgaz, 1994) and orange (Castel, 2001) (Table S3 [suppl.]).

Results

Absolute minimum temperature (tminabs) data

To perform agroclimatic analyses following Papadakis' approach, three of the four required variables (average monthly Tmax, tmin and P) were already publicly available from the DCAC, but data layers for the additionally required variable (average monthly tminabs) were generated in this work. The four independent variables (Alt, DistSea, CosLat, and Rad) showed behaviours and correlation coefficients (Table S4 [suppl.]) comparable to those of other DCAC thermal data layers. Maps of tminabs for the 12 months of the year were obtained using the UK interpolation technique (Fig. S1 [suppl.]), which had a RMSE error between 1.13 and 1.69 ºC, lower than multiple regression (Table S5 [suppl.]).

Papadakis' agroclimatic zoning

In the baseline scenario, the warm and cool maritime thermal regimes occupied each approx. 40% of the surface of Catalonia and coincided with semi-arid agricultural areas in the interior (which is very dependent on irrigation) and the coast (which has a tradition for several rainfed crops). The cold maritime regime coincided approximately with the Pyrenees subregion and occupied more than 18% of the study area. There was also a fourth type, the semi-warm subtropical regime, present only in the Ebro Delta and in some sparse points in the southern half of the coast (Table 2).

As for the humidity regime, the Pyrenees subregion was found to have humid or humid Mediterranean regimes, the coastal subregion mostly dry Mediterranean, and the interior mostly semi-arid Mediterranean (Table 3).

When visualized as maps, the comparison between the baseline and future scenarios showed that the warm coastal zone will advance towards the interior as the colder regimes retreat, mainly due to the expansion of *Oryza* and *Gossypium* summer types and the *Citrus* winter type (Fig. 3), which will push colder types inland. Simultaneously, the semi-arid Mediterranean humidity regime will expand from the interior towards the coast as humid regimes recede remarkably toward higher altitudes.

Table 2. Definition and percentage of territory occupied by each thermal regime in the baseline and future scenarios under study.

	Type of winter[1,3]	Type of summer[2,3]	Area 1971-2000 (%)	Area 2031-2050 (%)
Semi-warm subtropical	Ci or cooler	g or warmer	1.2	21.3
Warm maritime	Ci or cooler	O, M	39.7	40.5
Cool maritime	av or cooler	T or warmer	40.8	28.2
Cold maritime	av/Ti	P or warmer	17.3	9.8
Other			1.0	0.2

[1] Ci=cool *Citrus*; av=cool *Avena*; Ti=warm *Triticum*; g=cool *Gossypium*. [2] O=*Oryza*; M=maize; T=*Triticum*; *P*=polar. [3] The definitions of types of winter and summer are provided in Table S1 [suppl.].

Table 3. Percentage of territory occupied by each humidity regime in the baseline and future scenarios under study.

	Area 1971-2000 (%)	Area 2031-2050 (%)
Permanently humid	8.1	5.3
Humid	6.4	4.3
Humid Mediterranean	20.2	15.3
Dry Mediterranean	35.8	30.2
Semi-arid Mediterranean	29.6	45.0

The definitions of humidity regimes are provided in Table S1 [suppl.].

Suitability of cultivation

The impact of the changes described in temperature and moisture conditions was evaluated by calculating the suitability of five typical Mediterranean crops which together represent about 45% of the cultivated land in Catalonia, according to the 2018 Single Agrarian Declaration (DUN2019) (Table S6 [suppl.]).

Initially, the performance of Papadakis' methodology as an instrument for predicting the potential distribution of crops was evaluated by calculating the percent coincidence between the existence of a crop and Papadakis' suitability class at the corresponding location. In the year 2018, 100% of the registered fields growing alfalfa, barley and olive trees were located in areas where winter and summer types are suitable for the corresponding crop according to Papadakis (*i.e.*, none of these traditional crops are grown in areas that Papadakis' classification would consider inadequate for the crop) (Table 4). A more recently established crop, orange, showed a rate of coincidence above 90%. In contrast, the viability of almond seems to be poorly predicted by this classification system (nearly 40% of present-day almond orchards are in areas that Papadakis' method would consider too cold, as discussed below).

When climate suitability of the five species was visualized as maps (this time taking into account humidity along with thermal regimes), the current real distribution of crops was found to largely reflect these agroclimatic computations (Fig. 4). However, two apparent contradictions may be observed, caused by water availability (rather than need) and the presence of varieties adapted to local climates.

On the one hand, in the Littoral subregion, barley is grown with irrigation in locations where these crops would be suitable in the drylands, just because irrigation is readily available in these areas. On the other hand, in the Interior subregion some almond plantations exist which, according to Papadakis' categorization, are in an excessively cold area. This fact probably indicates a limitation of Papadakis' system to predict the viability of almond cultivars, some of which can withstand harsher winters than the coldest category that can be reasonably applied (*i.e.*, almond withstands *warm Avena* winters or warmer; some cultivars may withstand the milder versions of the *cool Avena* category, above a threshold that is not discerned by this classification).

This procedure was then applied to compare agroclimatic suitability for the baseline scenario and the 2031-50 scenario. No transitions from V to NV or V_{irr} to NV were detected for any of the studied crops, but the opposite changes (NV to V or NV to V_{irr}) do take place (Table 5). Therefore, the change to warmer winter and summer conditions will not reduce the viability area of any of the crops, but it will enable some of them to be grown in areas that have been traditionally too cold for them, as long as water demands are covered. On the other hand, for most crops the transitions V to V_{irr} and NV to V_{irr} are abundant, mainly due to the expansion of the semi-arid Mediterranean regime and the retraction of the humid Mediterranean regime (Fig. 3 and Table 5). The woody crops (almond, orange and olive trees) are the species that gain larger potential cultivation areas (19.4%, 12.2% and 7.2% of the study area, respectively).

Upon inspection of these data as maps, it appeared that the suitability of almond will increase thanks to irrigation

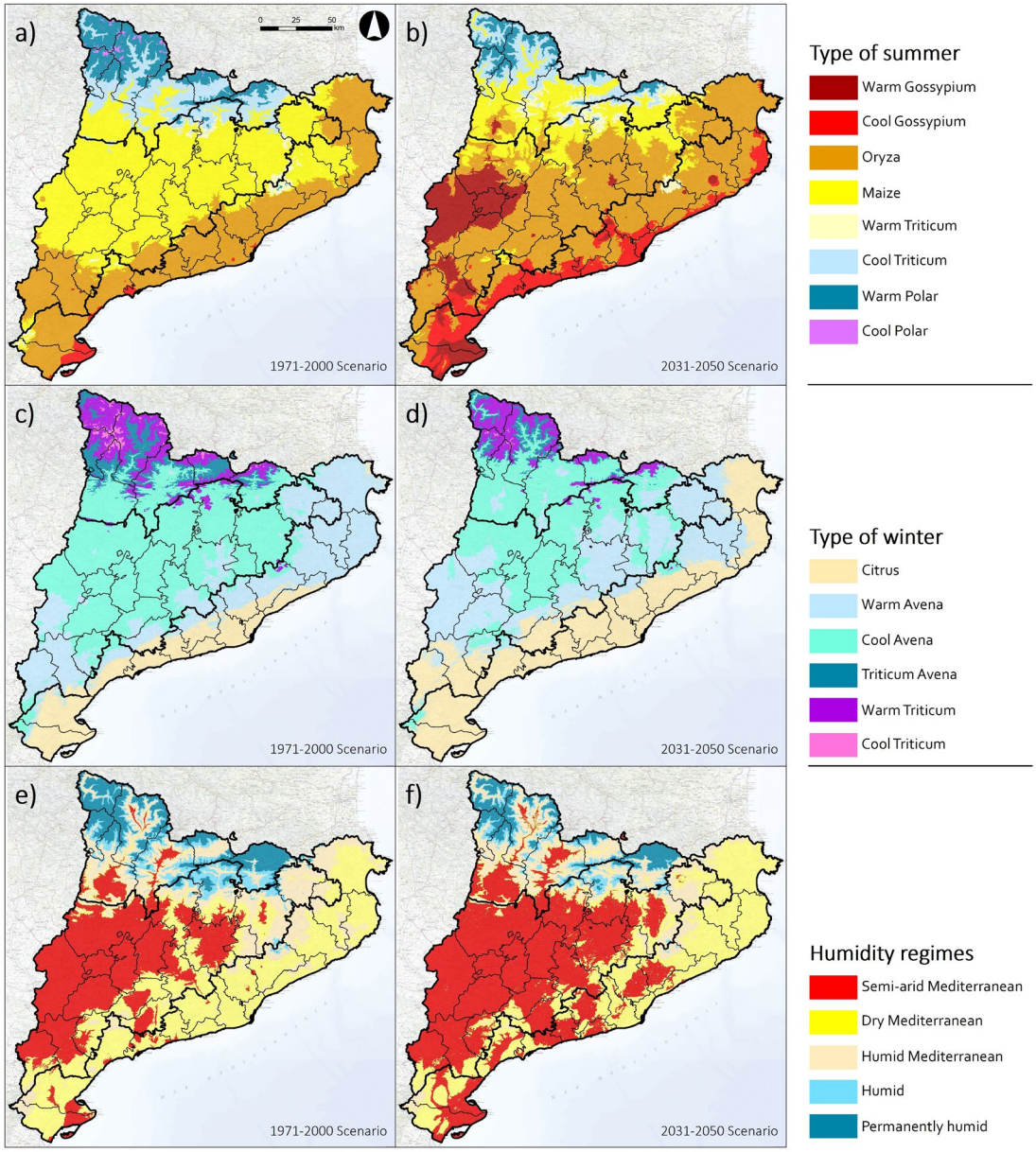

Figure 3. Maps of summer and winter types and humidity regime according to Papadakis in the baseline and future scenarios.

Table 4. Percentage of coincidence with Papadakis thermal suitability for each of the five selected crops over the study area.

	Area DUN2019 (ha)	% area DUN	% coincidence
Alfalfa	32,756.0	4.7	100.0
Almond	33,268.9	4.8	62.9
Olive	86,837.3	12.4	100.0
Barley	171,070.6	24.5	100.0
Orange	1,702.9	0.5	90.6

The definitions of humidity regimes are provided in Table S1 [suppl.].

(19.4%) in highland areas of the plains and inland mountains (Fig. 5, Table 5). Nevertheless, an important part of the study area (39.6%) will remain unsuitable for this crop, except for some late-flowering varieties that may be suited for slightly colder conditions than those of the coldest Papadakis categories that can be applied. Orange trees may become a viable crop along almost the entire Catalan coast in the next few decades, as long as irrigation is a possibility. In general terms, however, 86.6% of the study area will remain unsuitable for orange growing (Fig. 5e, Table 5). Olive trees will still be suitable as a rainfed crop on 41.8% of the land, while if irrigation is provided they will be viable in an additional 44.9% of the area. This implies an increase of 15.4% in areas in which irrigation would be mandatory for olive production.

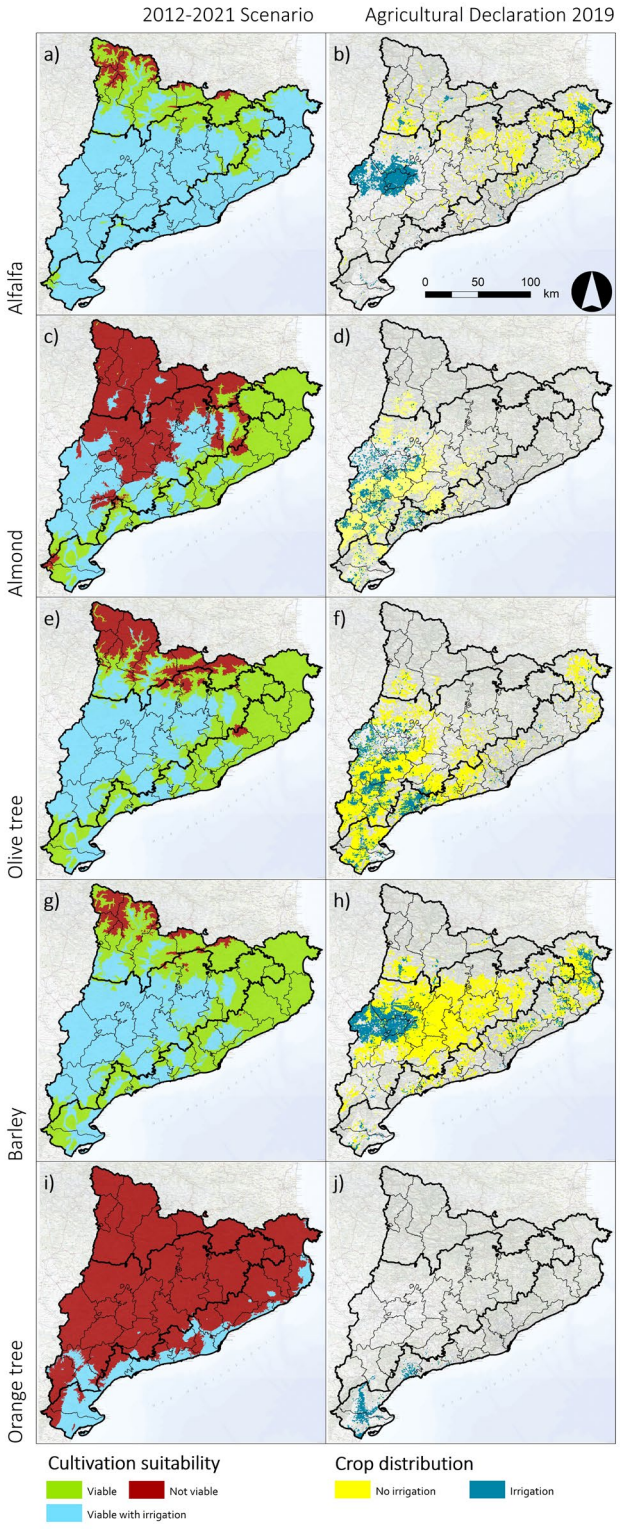

Figure 4. Left panel: Cultivation suitability of the five targeted crops in the 2012-21 scenario. Green, blue and red indicate V, V_{irr} and NV, respectively. Right panel: Actual fields in which each crop is grown with (blue) or without (yellow) irrigation.

Regarding herbaceous crops, barley will maintain a larger area of cultivation suitability without irrigation (49.6%), although 45% of the land will require irrigation and, in the timeframe under study, this land will increase by 15.4%. This will inevitably lead to a drop of productivity in many of the areas that need irrigation, since barley production has a meagre economic margin and is often not worth irrigating. Alfalfa will have a larger area requiring irrigation (a 9.8% increase), which will reach 75.1% of the land. As with barley, in many areas of the country, rainfed lands will presumably be less productive for alfalfa compared to the present day.

Combined water deficit of the five species under study

In order to quantify the increasing difficulties of cultivation conditions in terms of water stress, the water deficit of all irrigated fields of the DUN2019 that contain one of the five target crops was calculated, and water requirement of every irrigated field according to its surface was obtained. This subset added up to 67,535 fields (82,850 ha) and therefore constituted about 11.5% of the total farmland of Catalonia and one third of the total irrigated fields according to the DUN2019 (Table S6 [suppl.]).

The combined water demand of the fields that currently have one of the five crops under irrigation will increase by more than 16% between the base and future scenarios, going from 330 to 383 hm^3 (Table 6). Percentage-wise, this increase in water demand will be more pronounced in coastal areas and the Pyrenees, although most of the consumption will continue to be in the Interior subregion (more than 80%), largely due to alfalfa and barley (Table S7 [suppl.]).

Discussion

The calculation of tminabs following previously established methodology generated results with a statistical significance comparable to that of other layers of information already published (Ninyerola *et al.*, 2000); therefore, it provides a solid basis for subsequent agroclimatic studies. The fact that UK is superior to multiple linear regression as an interpolation method for climate variables has been observed previously (Bostan *et al.*, 2012).

Papadakis' classification was chosen as a well-known procedure to visualize the agricultural potential of a region's climate. The current distribution of crops in the study area was found to fit Papadakis' thermal suitability predictions in four out of the five selected species. In combination with climate change projections, this methodology enabled the visualization and quantification of the impacts of climate change on agriculture in the region.

Agroclimatic zoning of baseline and future scenarios showed that a substantial increase in subtropical thermal regime (+20.1%) and a drastic reduction of cool and cold maritime regimes (-20.1% taken together) will

Table 5. Percentage of territory occupied by each combination of suitability in the baseline scenario and suitability in the future scenario for the studied crops. The last three rows are the result of operating with the rows above (M=E+G-B-J; N=-C+G-I-J; O=M-N).

Suitability 1971-2000	Suitability 2031-2050	Alfalfa	Almond	Olive	Barley	Orange	Row
V	V	16.6	24.0	34.1	45.4	0.0	A
V_{irr}	V	0.0	0.6	0.8	0.8	0.0	B
NV	V	4.7	6.2	6.9	3.3	0.0	C
	Subtot 31-50	21.2	30.9	41.8	49.6	0.0	D
V	V_{irr}	9.7	8.0	15.9	16.2	0.0	E
V_{irr}	V_{irr}	65.4	8.3	28.7	28.8	1.2	F
NV	V_{irr}	0.0	13.2	0.3	0.0	12.2	G
	Subtot 31-50	75.1	29.5	44.9	45.0	13.4	H
V	NV	0.0	0.0	0.0	0.0	0.0	I
V_{irr}	NV	0.0	0.0	0.0	0.0	0.0	J
NV	NV	3.6	39.6	13.3	5.4	86.6	K
	Subtot 31-50	3.6	39.6	13.3	5.4	86.6	L
Sum		100.0	100.0	100.0	100.0	100.0	
New irrigation area		9.8%	20.6	15.4	15.4	12.2	M
New viability area		4.7%	19.4	7.2	3.3	12.2	N
Dryland viability loss		5.1%	1.1	8.2	12.0	0.0	O

occur, accompanied by the expansion of the semi-arid Mediterranean humidity regime (which will become the most common regime in the future scenario). Our results for the baseline scenario are comparable to the Papadakis climate layers available at the SIGA agricultural data viewer (Spanish Ministry of Agriculture, 2012), which have a lower resolution than those used in the present study.

As a consequence of these changes, the majority of crops will be viable in larger areas, but the new high-altitude areas with a higher rainfall (where cultivation suitability changes from NV to V) will not quite compensate the increase of the areas in which irrigation will become mandatory. Therefore, all crops will have a larger potential cultivation area, but they will be more dependent on irrigation availability. Irrigation is known to decrease sensitivity to heat stress, and for some areas and crops, warmer conditions may lead to increased yields, as long as water needs are met (Zaveri & Lobell, 2019).

The changes in humidity regime will bring about an increase in water demand of the studied crops (together representing about a third of the irrigated land of Catalonia) of about 16% on average. In absolute terms, the increase of 53 hm^3 to irrigate the five targeted species are comparable to the increase of 197 hm^3 for the total irrigated land of Catalonia predicted in the TRCCC (Sebastià *et al.*, 2016). Most of the water consumption of these species (> 80%) will continue to be in the Interior, which is where most of the irrigation infrastructure in Catalonia is found. Through improved water-management and irrigation techniques, however, reductions of water use of up to 40% can be achieved (Kourgialas *et al.*, 2019).

It should be noted that in regional predictive models of climate change, precipitation projections of each season have a greater uncertainty than temperature projections (Gonçalves *et al.*, 2014). The need for better rainfall predictive models to improve agricultural performance predictions has been underscored in multiple studies (Watson & Chalinor, 2013; Ullah *et al.*, 2017). In addition, Papadakis' methodology assumes a soil water carrying capacity of 100 mm if real values are unknown. When sound high-resolution data for this variable become available, the methodology followed in this study will generate more precise predictions of evapotranspiration, and therefore of humidity regime and water deficit (Folberth *et al.*, 2016). A high-resolution soil map of Catalonia is currently under development (ICGC, 2019), which will enable the estimation of soil water carrying capacity all over the region.

Climate change, therefore, can significantly affect the distribution of crops in Catalonia and generate structural changes in production. With continued improvement of data and modelling, priority areas and types of interventions can be defined with a very detailed resolution. Herbaceous and woody crops may use different adaptation strategies. For almonds, the poor performance of Papadakis' methodology to predict present-day orchards may reflect an ongoing adaptation to climate change: old orchards are being abandoned or replaced with hybrids adapted to shorter cold seasons and late-flowering varieties that enable harvest in mountainous areas (Vargas *et al.*, 2008), where

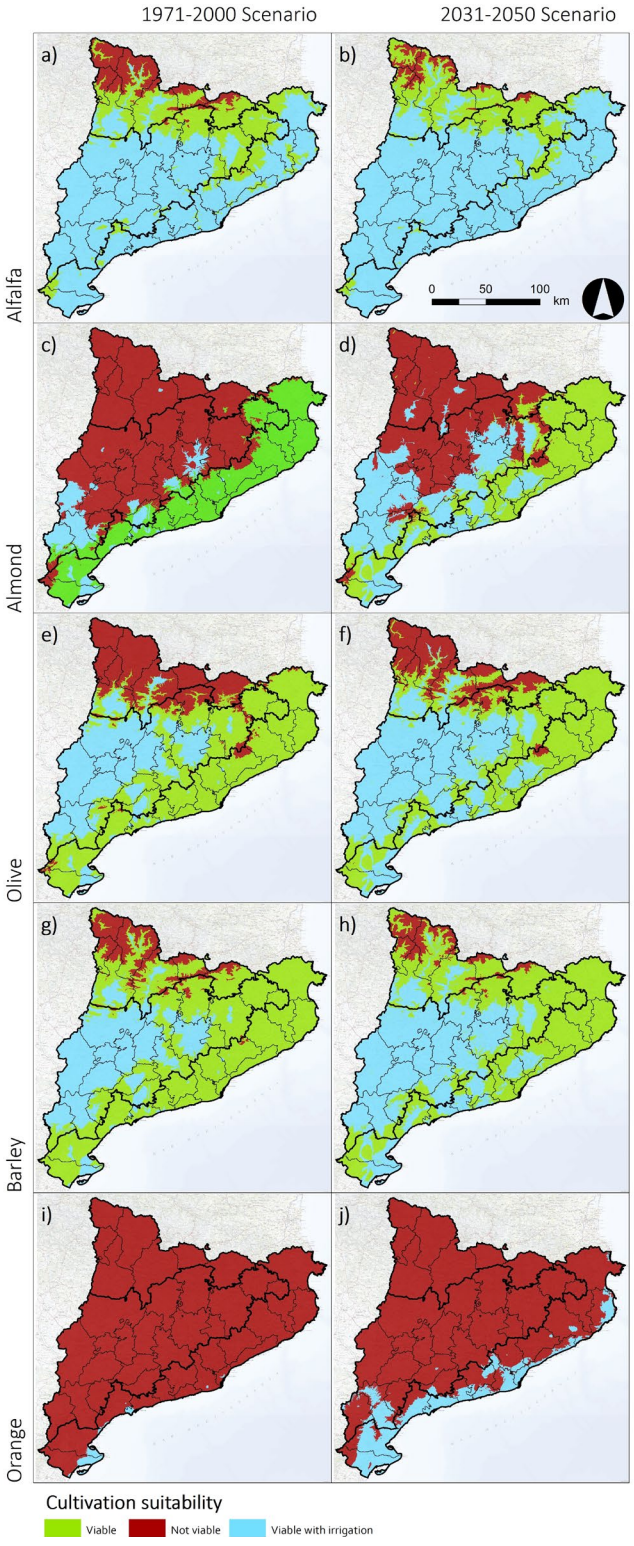

Figure 5. Cultivation suitability of the five targeted crops in the baseline (left) and future (right) scenarios. Green, blue and red indicate V, V_{irr} and NV, respectively.

almonds can still be produced as a rainfed crop. Oranges are predicted to have a large expansion potential; however, this new potential cultivation area is restricted to the coast, where urban uses of water and land are greatest and new irrigation developments are unlikely. Therefore, the current citric production areas will remain viable with irrigation, but the expansion of this crop will depend on strongly determining factors beyond climate suitability. On the other hand, olive trees will have a larger potential cultivation area with extended growing seasons (Benlloch-González *et al.*, 2018); however, in certain areas of the Western Mediterranean a loss of productivity is expected due to increased water stress (Fraga *et al.*, 2019). The remarkable expansion of suitable olive-growing areas with a strong dependence on irrigation observed in this study is consistent with previous studies with a European scope (Tanasijevic *et al.*, 2014). Regarding herbaceous crops, barley has traditionally been grown during winter and spring, and it is likely to be strongly affected by the decreased spring precipitation. Rainfed barley fields may require the use cultivars suited for early autumn sowing and early spring harvest, given that this species is more sensitive to water deficiency and temperature extremes in the early stages of its growth cycle (Cammarano *et al.*, 2019). Alfalfa has higher water requirements; in areas were precipitation is sufficient, the increased temperature and CO_2 concentration may benefit productivity (Thivierge *et al.*, 2016), but these environments will be restricted to the Pyrenees mountain range, and this crop will require irrigation in most of the study area.

In irrigated areas, if sufficient water resources are available, the impacts on production and crop replacement may be lower, but efficient water-management systems will be needed. In traditional rainfed agriculture areas, especially the coastal and inland locations South of Barcelona, these impacts are likely to be drastic, and a substitution of crops or the establishment of support irrigation systems must be considered to avoid a significant drop in productivity, as suggested by a simulation of rainfed crop yield that covers all of Europe at a lower resolution for the 2030 time-horizon (Donatelli *et al.*, 2015). The transition to warmer conditions will also favour some pests associated with the different crops, which may influence the adaptive response, economic viability and productive area (Ponti *et al.*, 2014). In some instances, however, pests may be negatively influenced by warmer conditions and advanced flowering times (Aurambout *et al.*, 2009). In the Pyrenees subregion, some Mediterranean crops may become interesting new options, relative to alfalfa and other animal fodder that are currently grown. However, even in these mountainous regions, some varieties will need irrigation due to the strong Mediterraneanisation of the area. In addition, the higher frequency of extreme phenomena (warm nights, extreme temperatures and precipitation) that are expected in the study area (Barrera-Escoda *et al.*, 2014) can have a stronger negative impact than the changes in average temperatures and precipitation (Trnka *et al.*, 2015; Ullah *et al.*, 2017). Most importantly, multiple social and economic factors determining adaptive capacity will lead to different impacts of climate change in

Table 6. Water deficit (WD) of irrigated (R) and dryland fields (S) with one of the five targeted crops in the base scenario (mm, average ± SD), increase estimated for the 2031-50 scenario (var WD), total gross irrigation needs (gIN) in the baseline and future scenarios (hm^3), and percent-increase of the total gIN.

	WD 1971 (mm)		Var WD (mm)		gIN 1971 (hm^3)	gIN 2031 (hm^3)	Increase gIN (%)
	R	S	R	S	R	R	R
Interior	420.68 ± 160.35	290.71 ± 106.17	66.19 ± 17.92	57.20 ± 17.01	271.66	311.99	14.8
Littoral	294.83 ± 118.23	256.33 ± 85.43	72.81 ± 17.17	69.41 ± 16.20	50.96	63.44	24.5
Pyrenees	351.78 ± 181.92	234.72 ± 112.59	69.81 ± 27.83	66.38 ± 23.95	6.65	7.95	19.5
Total 5 crops					**329.27**	**383.38**	**16.4**

different areas (Kahil *et al.*, 2015; Parker *et al.*, 2019). The highest-altitude areas, above 1500 m, will remain clearly inhospitable for agriculture.

The case-study presented here underscores the importance of improved predictions of seasonal precipitation and temperature changes for local agricultural planning and recovers a classical methodology to evaluate the impact of these changes on climatic suitability of common crops. The procedure used in this work enables the detection of climate-derived risks and opportunities for the agricultural sector with a high spatial resolution.

Acknowledgments

We wish to thank the Catalan Meteorological Service for providing meteorological station records of absolute minimum temperature, and Mr. Gabriel Borràs Calvo for his constructive comments on the manuscript.

References

Allen RG, Pereira LS, Raes D, Smith M, 1998. Crop evapotranspiration. Guidelines for computing crop water requirements. FAO Irrig Drain paper 56.

Aurambout JP, Finlay KJ, Luck J, Beattie GAC, 2009. A concept model to estimate the potential distribution of the Asiatic citrus psyllid (*Diaphorina citri Kuwayama*) in Australia under climate change-A means for assessing biosecurity risk. Ecol Model 220: 2512-2524. https://doi.org/10.1016/j.ecolmodel.2009.05.010

Barrera-Escoda A, Gonçalves M, Guerreiro D, Cunillera J, Baldasano JM, 2014. Projections of temperature and precipitation extremes in the North Western Mediterranean basin by dynamical downscaling of climate scenarios at high resolution (1971-2050). Climatic Change 122: 567-582. https://doi.org/10.1007/s10584-013-1027-6

Benavides R, Montes F, Rubio A, Osoro K, 2007. Geostatistical modelling of air temperature in a mountainous region of Northern Spain. Agr Forest Meteorol 146: 173-188. https://doi.org/10.1016/j.agrformet.2007.05.014

Benlloch-González M, Sanchez-Lucas R, Benlloch M, Fernández-Escobar R, 2018. An approach to global warming effects on flowering and fruit set of olive trees growing under field conditions. Sci Hortic 240: 405-410. https://doi.org/10.1016/j.scienta.2018.06.054

Bostan PA, Heuvelink GBM, Akyurek SZ, 2012. Comparison of regression and kriging techniques for mapping the average annual precipitation of Turkey. Int J Appl Earth Observ Geoinform 19: 115-126. https://doi.org/10.1016/j.jag.2012.04.010

Brouwer C, Heibloem M, 1986. Irrigation water management: Irrigation water needs. Training Manual, FAO, Rome.

Calbó J, Gonçalves M, Barrera A, García-Serrano J, Doblas-Reyes F, Guemas V, Cunillera J, Altava V, 2016. Projeccions climàtiques i escenaris de futur. In: Tercer Informe Del Canvi Climàtic a Catalunya. Institut d'Estudis Catalans & Generalitat de Catalunya, Barcelona, pp: 113-133.

Cammarano D, Ceccarelli S, Grando S, Romagosa I, Benbelkacem A, Akar T, Ronga D, 2019. The impact of climate change on barley yield in the Mediterranean basin. Eur J Agron 106: 1-11. https://doi.org/10.1016/j.eja.2019.03.002

Castel J, 2001. Consumo de agua por plantaciones de cítricos en Valencia. Nutrifitos 77: 27-32.

De Leon Llamazares A, 1989. Caracterización agroclimática de las provincias de Tarragona, Barcelona, Lleida y Girona. Madrid: Ministerio de Agricultura Pesca y Alimentación. https://www.mapa.gob.es/ministerio/pags/Biblioteca/fondo/pdf/2884_all.pdf [11.25.19].

Donatelli M, Srivastava AK, Duveiller G, Niemeyer S, Fumagalli D, 2015. Climate change impact and potential adaptation strategies under alternate realizations of climate scenarios for three major crops in Europe. Environ Res Letters 10: 075005. https://doi.org/10.1088/1748-9326/10/7/075005

FAO, 2002. Crop water requirements and irrigation scheduling. In: FAO Irrigation Manual Module 4; Savva AP & and Frenken K (eds.), Rome.

Ferrise R, Moriondo M, Trombi G, Miglietta F, Bindi M, 2013. Climate change impacts on typical mediterranean crops and evaluation of adaptation strategies to cope with. In: Regional assessment of climate change in the Mediterranean; Navarra A & Tubiana L (eds). Adv Global Change Res 51. Springer, Dordrecht, pp: 49-70. https://doi.org/10.1007/978-94-007-5772-1_4

Folberth C, Skalský R, Moltchanova E, *et al.* (2016). Uncertainty in soil data can outweigh climate impact signals in global crop yield simulations. Nat Commun 7: 11872. https://doi.org/10.1038/ncomms11872

Fraga H, Pinto JG, Viola F, Santos JA, 2019. Climate change projections for olive yields in the Mediterranean Basin. Int J Climatol 40: 769-781. https://doi.org/10.1002/joc.6237

Garrido A, Rey D, Ruiz-Ramos M, Mínguez MI, 2011. Climate change and crop adaptation in Spain: consistency of regional climate models. Climate Res 49: 211-227. https://doi.org/10.3354/cr01029

Gonçalves M, Barrera-Escoda A, Guerreiro D, Baldasano JM, Cunillera J, 2014. Seasonal to yearly assessment of temperature and precipitation trends in the North Western Mediterranean Basin by dynamical downscaling of climate scenarios at high resolution (1971-2050). Climatic Change 122: 243-256. https://doi.org/10.1007/s10584-013-0994-y

Hengl T, Heuvelink GBM, Rossiter DG, 2007. About regression-kriging: From equations to case studies. Comput Geosci 33: 1301-1315. https://doi.org/10.1016/j.cageo.2007.05.001

ICGC 2019. Descripció del mapa de sòls 1:25.000. https://www.icgc.cat/Administracio-i-empresa/Serveis/Sols/Descripcio-del-Mapa-de-sols-1-25.000 [11.25.19].

Kahil MT, Connor JD, Albiac J, 2015. Efficient water management policies for irrigation adaptation to climate change in Southern Europe. Ecol Econ 120: 226-233. https://doi.org/10.1016/j.ecolecon.2015.11.004

Kourgialas NN, Koubouris GC, Dokou Z, 2019. Optimal irrigation planning for addressing current or future water scarcity in Mediterranean tree crops. Sci Total Environ 654: 616-632. https://doi.org/10.1016/j.scitotenv.2018.11.118

Ninyerola M, Pons X, Roure JM, 2000. A methodological approach of climatological modelling of air temperature and precipitation through GIS techniques. Int J Clim 20: 1823-1841. https://doi.org/10.1002/1097-0088(20001130)20:14<1823::AID-JOC566>3.0.CO;2-B

Papadakis J, 1966. Climates of the world and their agricultural potentialities. Buenos Aires.

Parker L, Bourgoin C, Martinez-Valle A, Läderach P, 2019. Vulnerability of the agricultural sector to climate change: The development of a pan-tropical climate risk vulnerability assessment to inform sub-national decision making. PLoS One14 (3): e0213641. https://doi.org/10.1371/journal.pone.0213641

Pascual D, Zabalza Martinez J, Funes I, Vicente-Serrano S, Pla E, Aranda X, Save R, Biel C, 2016. Impacts of climate and global change on the environmental hydrological and agriculture systems in the LIFE MEDACC case study basins. Deliverable 14. LIFE MEDACC.

Pastor M, Orgaz F, 1994. Riego deficitario del olivar. Agricultura 746: 768-776.

Peñuelas J, Boada M, 2003. A global change-induced biome shift in the Montseny mountains (NE Spain). Global Change Biol 9: 131-140. https://doi.org/10.1046/j.1365-2486.2003.00566.x

Ponti L, Gutierrez AP, Ruti PM, Dell'Aquila A, 2014. Fine-scale ecological and economic assessment of climate change on olive in the Mediterranean Basin reveals winners and losers. Proc Nat Acad Sci 111: 5598-5603. https://doi.org/10.1073/pnas.1314437111

Quiroga S, Iglesias A, 2009. A comparison of the climate risks of cereal citrus grapevine and olive production in Spain. Agr Syst 101: 91-100. https://doi.org/10.1016/j.agsy.2009.03.006

Ronchail J, Cohen M, Alonso-Roldan M, Garcin H, Sultan B, Angles S, 2014. Adaptability of Mediterranean agricultural systems to climate change: the example of the Sierra Magina olive-growing region (Andalusia, Spain). Part II: the future. Weather Clim Soc 6 (4): 451-467. https://doi.org/10.1175/WCAS-D-12-00045.1

Saadi S, Todorovic M, Tanasijevic L, Pereira LS, Pizzigalli C, Lionello P, 2015. Climate change and Mediterranean agriculture: impacts on winter wheat and tomato crop evapotranspiration, irrigation requirements and yield. Agr Water Manage 147: 103-115. https://doi.org/10.1016/j.agwat.2014.05.008

Sebastià MT, Plaixats-Boixadera J, Lloveras J, Girona J, Caiola Nuno Savé R, 2016. Sistemes agroalimentaris: agricultura ramaderia i pesca. In: Tercer Informe Del Canvi Climàtic a Catalunya. Institut d'Estudis Catalans & Generalitat de Catalunya, Barcelona, pp: 315-336.

Spanish Ministry of Agriculture, 2012. Sistema de información geográfica de datos agrarios. https://sig.mapama.gob.es/siga/ [11.25.19].

Tanasijevic L, Todorovic M, Pereira L.S, Pizzigalli C, Lionello P, 2014. Impacts of climate change on olive crop evapotranspiration and irrigation requirements in the Mediterranean region. Agr Water Manage 144: 54-68. https://doi.org/10.1016/j.agwat.2014.05.019

Thivierge MN, Jégo G, Bélanger G, Bertrand A, Tremblay GF, Rotz CA, Qian B, 2016. Predicted yield and nutritive value of an alfalfa-timothy mixture under climate change and elevated atmospheric carbon dioxide. Agron J 108: 585-603. https://doi.org/10.2134/agronj2015.0484

Trnka M, Hlavinka P, Semenov MA, 2015. Adaptation options for wheat in Europe will be limited by increased adverse weather events under climate change. J R Soc Interface 12: 20150721. https://doi.org/10.1098/rsif.2015.0721

Ullah A, Ashfaq A, Tasneem K, Javaid A, 2017. Recognizing production options for pearl millet in Pakistan under changing climate scenarios. J Integr Agr 16: 762-773. https://doi.org/10.1016/S2095-3119(16)61450-8

Vargas F, Romero M, Clavé J, Vergés J, Santos J, Batlle I, 2008. "Vayro",'Marinada','Constantí', and "Tarraco" Almonds. Hortic Sci 43: 535-537. https://doi.org/10.21273/HORTSCI.43.2.535

Verheye W, 2008. Agro-climate based land evaluation systems. In: Land use land cover and soil sciences; Verheye W (Ed.). UNESCO-EOLSS Publ, Oxford, UK.

Watson J, Challinor AJ, 2013. The relative importance of rainfall, temperature and yield data for a reginal-scale crop model. Agr Forest Meteorol 170: 47-57. https://doi.org/10.1016/j.agrformet.2012.08.001

Zaveri EB, Lobell D, 2019. The role of irrigation in changing wheat yields and heat sensitivity in India. Nature Commun 10: 4144. https://doi.org/10.1038/s41467-019-12183-9